

C. Guignabert, C. M. Alvira, T.-P. Alastalo, H. Sawada, G. Hansmann, M. Zhao, L. Wang, N. El-Bizri and M. Rabinovitch

Am J Physiol Lung Cell Mol Physiol 297:1082-1090, 2009. First published Oct 2, 2009;
doi:10.1152/ajplung.00199.2009

You might find this additional information useful...

Supplemental material for this article can be found at:

<http://ajplung.physiology.org/cgi/content/full/00199.2009/DC1>

This article cites 46 articles, 23 of which you can access free at:

<http://ajplung.physiology.org/cgi/content/full/297/6/L1082#BIBL>

Updated information and services including high-resolution figures, can be found at:

<http://ajplung.physiology.org/cgi/content/full/297/6/L1082>

Additional material and information about *AJP - Lung Cellular and Molecular Physiology* can be found at:

<http://www.the-aps.org/publications/ajplung>

This information is current as of November 26, 2009 .

Tie2-mediated loss of peroxisome proliferator-activated receptor- γ in mice causes PDGF receptor- β -dependent pulmonary arterial muscularization

C. Guignabert,^{1,2} C. M. Alvira,^{1,2} T.-P. Alastalo,^{1,2} H. Sawada,^{1,2} G. Hansmann,^{1,2,3} M. Zhao,² L. Wang,^{1,2} N. El-Bizri,^{1,2} and M. Rabinovitch^{1,2}

¹Cardiopulmonary Research Program, Vera Moulton Wall Center for Pulmonary Vascular Disease, and Departments of ²Pediatrics (Cardiology) and ³Medicine, Stanford University School of Medicine, Stanford, California

Submitted 15 June 2009; accepted in final form 29 September 2009

Guignabert C, Alvira CM, Alastalo T-P, Sawada H, Hansmann G, Zhao M, Wang L, El-Bizri N, Rabinovitch M. Tie2-mediated loss of peroxisome proliferator-activated receptor- γ in mice causes PDGF receptor- β -dependent pulmonary arterial muscularization. *Am J Physiol Lung Cell Mol Physiol* 297: L1082–L1090, 2009. First published October 2, 2009; doi:10.1152/ajplung.00199.2009.—Peroxisome proliferator-activated receptor (PPAR)- γ is reduced in pulmonary arteries (PAs) of patients with PA hypertension (PAH), and we reported that deletion of PPAR- γ in smooth muscle cells (SMCs) of transgenic mice results in PAH. However, the sequelae of loss of PPAR- γ in PA endothelial cells (ECs) are unknown. Therefore, we bred Tie2-Cre mice with PPAR $\gamma^{\text{lox/lox}}$ mice to induce EC loss of PPAR- γ (Tie2 PPAR $\gamma^{-/-}$), and we assessed PAH by right ventricular systolic pressure (RVSP), RV hypertrophy (RVH), and muscularized distal PAs in room air (RA), after chronic hypoxia (CH), and after 4 wk of recovery in RA (Rec-RA). The Tie2 PPAR $\gamma^{-/-}$ mice developed spontaneous PAH in RA with increased RVSP, RVH, and muscularized PAs vs. wild type (WT); both genotypes exhibited a similar degree of PAH following chronic hypoxia, but Tie2 PPAR $\gamma^{-/-}$ mice had more residual PAH compared with WT mice after Rec-RA. The Tie2 PPAR $\gamma^{-/-}$ vs. WT mice in RA had increased platelet-derived growth factor receptor- β (PDGF-R β) expression and signaling, despite an elevation in the PPAR- γ target apolipoprotein E, an inhibitor of PDGF signaling. Inhibition of PDGF-R β signaling with imatinib, however, was sufficient to reverse the PAH observed in the Tie2 PPAR $\gamma^{-/-}$ mice. Thus the disruption of PPAR- γ signaling in EC is sufficient to cause mild PAH and to impair recovery from CH-induced PAH. Inhibition of heightened PDGF-R β signaling is sufficient to reverse PAH in this genetic model.

endothelial cells; platelet-derived growth factor receptor- β ; pulmonary remodeling; smooth muscle cell; platelet-derived growth factor

THE PEROXISOME PROLIFERATOR-ACTIVATED receptors (PPARs) belong to a family of three nuclear proteins [α , β (δ), and γ] that have tissue-specific overlapping functions as transcription factors (3, 6, 41, 43). PPAR- γ is highly expressed in normal pulmonary artery (PA) endothelial cells (ECs) but is appreciably reduced in both experimental and clinical pulmonary arterial hypertension (PAH; Refs. 1, 38). PPAR- γ has antiproliferative and proapoptotic effects in systemic arterial smooth muscle cells (SMCs; Refs. 9, 29), consistent with its function as a tumor suppressor gene (4, 34).

We previously created a mouse in which PPAR- γ was deleted in vascular SMCs by breeding a mouse expressing Cre downstream of the SM22 α promoter with a mouse in which the critical exons of PPAR- γ were flanked by LoxP sites. The

SM22 α PPAR $\gamma^{-/-}$ mice developed PAH as judged by elevated right ventricular systolic pressure (RVSP), right ventricular hypertrophy (RVH), and muscularization of distal vessels (10). We then showed that the mechanism is related to reduced levels of a target of PPAR- γ , apolipoprotein (apo)E, a molecule that inhibits PDGF-R β function by binding to low-density receptor-like protein-1 and by preventing the activation of the PDGF-R β (2, 14, 26, 47). We further established the relevance of this model to the pathology of clinical PAH by showing that bone morphogenetic protein receptor-II (BMPR-II) ligands modulate PPAR- γ activation and apoE production (10) and inhibit PDGF-BB-mediated pulmonary artery smooth muscle cells (PASMCs) proliferation. Moreover, dysfunction of BMPR-II, as is seen in familial and sporadic idiopathic PAH (19), causes loss of BMP-mediated inhibition of PDGF-BB-induced PASMC proliferation, a feature that can be rescued with a PPAR- γ agonist (10).

Recently, transgenic mice were created with a selective loss of PPAR- γ in ECs and some hematopoietic lineages by breeding a mouse expressing Cre under the regulation of the Tie2 promoter (17) with the PPAR $\gamma^{\text{lox/lox}}$ mouse (12). These Tie2 PPAR $\gamma^{-/-}$ mice have systemic hypertension but only when fed a high-salt diet (27). However, the sequelae of loss of PPAR- γ in ECs on pulmonary hemodynamics and vascular remodeling are unknown. In view of our previous study (10) in mice in which PPAR- γ was deleted in vascular SMCs and because PPAR- γ is reduced in both ECs and SMCs of PAH patients (1), we hypothesized that Tie2 PPAR $\gamma^{-/-}$ mice would also develop PAH and the associated vascular changes in room air and would have more severe PAH than wild-type (WT) mice following exposure to chronic hypoxia and after recovery in normoxia.

MATERIALS AND METHODS

Production of Tie2 PPAR- γ Transgenic Mice

To generate mice deficient in PPAR- γ in ECs (Tie2 PPAR $\gamma^{-/-}$), mice expressing Cre recombinase under the control of the Tie2 promoter (17) were bred with mice containing the critical exons of PPAR- γ flanked by LoxP sites (12) obtained from Jackson Laboratories (Bar Harbor, ME). All the mice were Cre gene positive. Tie2 PPAR $\gamma^{-/+}$ males and females were bred to derive Tie2 PPAR $\gamma^{+/+}$, Tie2 PPAR $\gamma^{-/+}$, and Tie2 PPAR $\gamma^{-/-}$ littermates for initial analyses and for further crossbreeding. Tie2 PPAR $\gamma^{-/-}$ and littermate WT mice were used ($n = 10$ /group of each genotype 5 males and 5 females). The mice were either studied in room air at 12 wk of age, or were exposed to hypoxia (10% oxygen) for 3 wk between 8–11 wk of age, or were exposed to hypoxia and then allowed a period of room air “recovery” for 4 wk as previously described (8). All the experimental protocols used in this study were approved by the Institutional Animal Care Committee at Stanford University and adhered to the published

Address for reprint requests and other correspondence: M. Rabinovitch, Vera Moulton Wall Center for Pulmonary Vascular Disease, Stanford Univ. School of Medicine, CCSR Bldg., Rm. 2245B, 269 Campus Drive, Stanford, CA 94305-5162 (e-mail: marlener@stanford.edu).

guidelines of the National Institutes of Health and the American Physiological Society.

Hemodynamic Measurements and Assessment of Pulmonary Vascular Changes

RVSP, RV dp/dt, and heart rate were measured in unventilated mice that were under isoflurane anaesthesia (1.5–2.5%, 2 l O₂/min.) using a closed chest technique, by introducing a 1.4-F Millar catheter into the jugular vein and directing it to the right ventricle (46). Systemic blood pressure was determined in conscious animals by a noninvasive computerized tail-cuff method and verified by catheterization of the left carotid artery while the animals were under isoflurane anaesthesia. Left ventricular fractional shortening and cardiac output were evaluated by echocardiography (8).

After the hemodynamic assessments were completed, heparinized blood was collected by direct cardiac puncture to analyze lipid profiles and to assess general metabolic effects of PPAR γ deletion in ECs or other Tie2-expressing cells, as described in the supplemental data for this article that are available online at the *Am J Physiol Lung Cell Mol Physiol* website. The mice were killed by exsanguination. The heart and lungs were then removed en bloc, and RVH was later evaluated by the Fulton index, i.e., weight of right ventricle/left ventricle plus septum (RV/LV+S; Ref. 22). The pulmonary circulation was flushed with 3 ml of PBS at 37°C, and the lungs were prepared for morphometric analyses by barium gelatin injection of the pulmonary circulation and formalin inflation-fixation of the lung as described in the supplemental data. Alternatively, the right lung was quickly harvested, immediately snap-frozen in liquid nitrogen, and kept at -80°C for Western immunoblot analysis and total RNA extraction, and the left lung was prepared as described in MATERIALS AND METHODS in the data supplement.

Morphometric analyses were performed on paraffin-embedded lung sections stained using elastic van Gieson or Movat pentachrome stains. The total number of peripheral arteries was calculated as a ratio of the number of arteries per 100 alveoli in each of 5–6 different $\times 20$ microscopic fields per section from each lung. Muscularization was assessed in 15 higher magnification fields/per mouse ($\times 40$ magnification) by calculating the proportion of fully and partially muscularized peripheral (alveolar duct and wall) pulmonary arteries to total peripheral PAs. All morphometric analyses were performed by one observer, blinded as to genotype and condition, i.e., room air, hypoxia, and recovery.

Real-Time Quantitative RT-PCR

Total RNA was isolated from frozen lungs or cultured cells using Trizol (Invitrogen, Carlsbad, CA) and RNeasy mini kit (Qiagen, Valencia, CA). Total RNA (2 μ g) was reverse-transcribed using Superscript II (Invitrogen, Carlsbad, CA) per manufacturer's instructions. Gene expression levels of PPAR γ were quantified using pre-verified Assays-on-Demand TaqMan primer/probe sets (Applied Biosystems, Foster City, CA) and normalized to 18S ribosomal RNA using the comparative Ct method.

Western Immunoblotting

Frozen tissue was homogenized, or cultured cells were lysed in ice-cold RIPA buffer containing protease and phosphatase inhibitors. Protein concentration was determined using protein assay reagent (Bio-Rad, Richmond, CA), and 50 μ g of protein extracts were resolved on 4–12% NuPage Bis-Tris gels and electrotransferred to PVDF membranes. The PVDF membranes were incubated in blocking buffer for 1 h at room temperature and then incubated overnight at 4°C with primary antibodies for PPAR γ (1:500; Santa Cruz Biotechnology, Santa Cruz, CA), apoE (1:500; Abcam, Cambridge, MA), phosphoERK1/2 (1:2,000; Cell Signaling Technology, Beverly, MA), total ERK1/2 (1:1,000; Cell Signaling Technology), caveolin-1 (1/

1,000; BD Biosciences, San Jose, CA), PDGF-B, (Santa Cruz Biotechnology), phosphoPDGF-R β (Tyr751; 1:500; Cell Signaling Technology), and PDGF-R β (1:4,000; Upstate Biotechnology, Lake Placid, NY). The membranes were then washed and incubated with either sheep anti-mouse (1:1,000) or donkey anti-rabbit (1:1,000) horseradish peroxidase-conjugated secondary antibodies. Autoradiographs were developed using the ECL kit (antibodies and kit from Amersham Biosciences, GE Healthcare UK Limited, Bucks, UK). Equal loading of protein was confirmed by blotting for β -actin. Relative band strength was determined by densitometry.

Immunohistochemistry

Immunohistochemical staining was performed following antigen retrieval on sections from lungs that were perfused with saline to remove blood and then fixed by perfusion with 10% formalin and embedded in paraffin. The antibodies used and their dilutions were anti-PPAR γ (1:200, BD Biosciences) and anti-PDGF-R β (1:500, Upstate Biotechnology). Labeling was detected with the use of the Vectastain ABC system (Vector Laboratories, Burlingame, CA) following the manufacturer's protocol, and all sections were counterstained with hematoxylin (Sigma-Aldrich, Mountain View, CA).

Nitric Oxide Synthase Activity and Endothelin-1 Assays

Nitric oxide synthase activity was estimated by the method of Yui et al. (44) in which the stable end-products nitrate/nitrite were estimated using the nitric oxide synthase assay kit (catalog no. 482702; Calbiochem) following the manufacturer's instructions. Plasma endothelin-1 (ET-1) was assessed by ELISA as previously described (10, 42).

Cell Culture

Cultured human PSMCs. The effects of recombinant apoE protein on PDGF-R β expression were studied in human PSMCs obtained from Lonza (Walkersville, MD) and cultured according to the manufacturer's recommendation. Growth synchronized cells (following 48-h starvation in media supplemented with 0.1% FBS) were exposed to recombinant apoE (1, 5, and 10 μ g/ml) in serum-free medium for 24 h before protein extraction, and the expression of PDGF-R β was determined by Western immunoblot as previously described (11).

Cultured murine pulmonary ECs. To determine the effect of loss of PPAR γ in the Tie2-expressing cells, the apoE expression was assessed in cultured pulmonary ECs (PECs) isolated from the Tie2 PPAR γ and WT mice. Murine PECs were isolated by digesting whole lung tissue with collagenase IA (0.5 mg/ml) for 45 min at 37°C. The cell suspension was filtered through 70- μ m filters and then centrifuged at 250 g for 5 min. The cell pellet was then washed and resuspended, and ECs were selectively cultured after incubation with magnetic beads (Dynabeads; Invitrogen, Carlsbad, CA) coated with anti-CD-31 antibody (11). Characterization of the cell culture after isolation was performed by labeling with Dil-conjugated Ac-LDL (Dil-Ac-LDL). Total RNA was extracted with TRIzol reagent from EC harvested from WT and Tie2 PPAR γ ^{-/-} mice, cDNA was synthesized, and gene expression of PPAR γ and apoE was determined by quantitative RT-PCR using TaqMan gene expression assays (Applied Biosystems). Total protein was harvested from pooled samples of WT and Tie2 PPAR γ ^{-/-} mice PEC and subjected to Western immunoblot to determine the expression of PPAR γ protein. In some experiments, WT murine PECs were maintained for 24 h at 1% O₂ in a hypoxia chamber (Billups-Rothenberg, Del Mar, CA), permitting monitoring of O₂ at 1% and CO₂ in room air range, or they were kept in room air.

Statistical Analysis

The number of animals used in each determination is given in RESULTS (see Figs. 1–5). To determine the differences between the Tie2 PPAR γ ^{-/-} and WT mice, unpaired Student *t*-tests were per-

formed. One-way ANOVA followed by Bonferroni's post hoc analysis was used to assess changes in a given genotype related to hypoxia and recovery vs. room air. A *P* value of 0.05 was considered statistically significant.

RESULTS

Decreased PPAR γ Protein in PECs Isolated from the Tie2-PPAR γ ^{-/-} Compared with WT Mice

Deletion of PPAR γ in Tie2-expressing cells resulted in a loss of PPAR γ mRNA and protein expressed by the PECs isolated from the Tie2-PPAR γ ^{-/-} vs. WT mice by quantitative RT-PCR (Fig. 1A) and by Western immunoblot (Fig. 1B). In addition, immunohistochemistry was performed on lung sections of Tie2-PPAR γ ^{-/-} and WT mice and demonstrated a similar PPAR γ immunostaining in the PASMCs from both the Tie2-PPAR γ ^{-/-} and WT mice but an absence of immunoreactivity in the ECs of the transgenic mice and in alveolar macrophages, cells that also express Tie2 (17, 24). Our PPAR γ immunohistochemical studies showed no significant difference in the PPAR γ expression in PASMCs contained in the distal pulmonary artery walls in the Tie2 PPAR γ ^{-/-} mice (Fig. 1C).

Tie2 PPAR γ ^{-/-} Mice Develop Mild PAH at Baseline and Impaired Recovery from Hypoxia-Induced PAH

An increase in RVSP (*P* < 0.001) was observed in Tie2 PPAR γ ^{-/-} compared with WT mice in room air, but a similar degree of RVSP elevation was induced in both genotypes by chronic hypoxia. However, following 4 wk of recovery in room air, the Tie2-PPAR γ ^{-/-} mice had higher residual RVSP than WT controls (28.5 ± 0.4 vs. 26.0 ± 0.3 mmHg, respectively; *n* = 10 in each group; *P* < 0.001; Fig. 2A). There were no significant differences between genotypes in heart rate, cardiac output, or left ventricular function (Table 1), although the Tie2 PPAR γ ^{-/-} mice did have higher triglycerides and triglyceride/HDL levels than WT mice (Supplemental Table S1). No

difference was observed in hematocrit values between genotypes (38.6 ± 1.4 vs. 40.5 ± 2.6 , respectively; *n* = 5 in each group; NS). Since PPAR γ suppresses asymmetric dimethyl-arginine and ET-1 (21, 23, 33, 37, 39), we measured nitric oxide production and ET-1 levels but no significant differences were observed between the genotypes (Supplemental Table S2).

Consistent with the RVSP values, greater RVH (RV/LV+S weight ratio) was found in the Tie2 PPAR γ ^{-/-} vs. WT mice (*P* < 0.05) in room air. A similar degree of RVH in both genotypes after chronic hypoxia, and persistent RVH in the Tie2 PPAR γ ^{-/-} mice compared with WT (*P* < 0.05) following 4 wk of recovery in room air (Fig. 2B). The elevation in RVSP and RVH in the Tie2 PPAR γ ^{-/-} mice at baseline were also associated with an increased number of muscularized distal pulmonary arteries vs. WT mice (*P* < 0.001; Fig. 2, C and D). Correlating with the similar elevation in RVSP and RVH following chronic hypoxia, there was a comparable increase in the percentage of muscularized distal arteries in both genotypes. The numbers of peripheral alveolar duct and wall arteries calculated relative to 100 alveoli in the two genotypes were not different in room air, in response to chronic hypoxia, and following recovery in room air (Table 1). For these, and all other assessments, no gender-related differences were observed, and each determination is based on similar numbers of male and female mice.

Several studies support the hypothesis that hypoxia induces changes in PPAR γ gene expression in different cell types. Recent findings by Nisbet et al. (28) show that in vitro hypoxia exposure (1% O₂ for 72 h) significantly reduced PPAR γ protein levels in both isolated human pulmonary artery ECs and smooth muscle cells. In addition, Li et al. (20) reported that compared with human proximal renal tubular epithelial cells under normoxic condition, amounts of PPAR γ mRNA were significantly decreased by 57% at 24 h and by 80% at 48 h in human proximal renal tubular epithelial cells under hypoxia

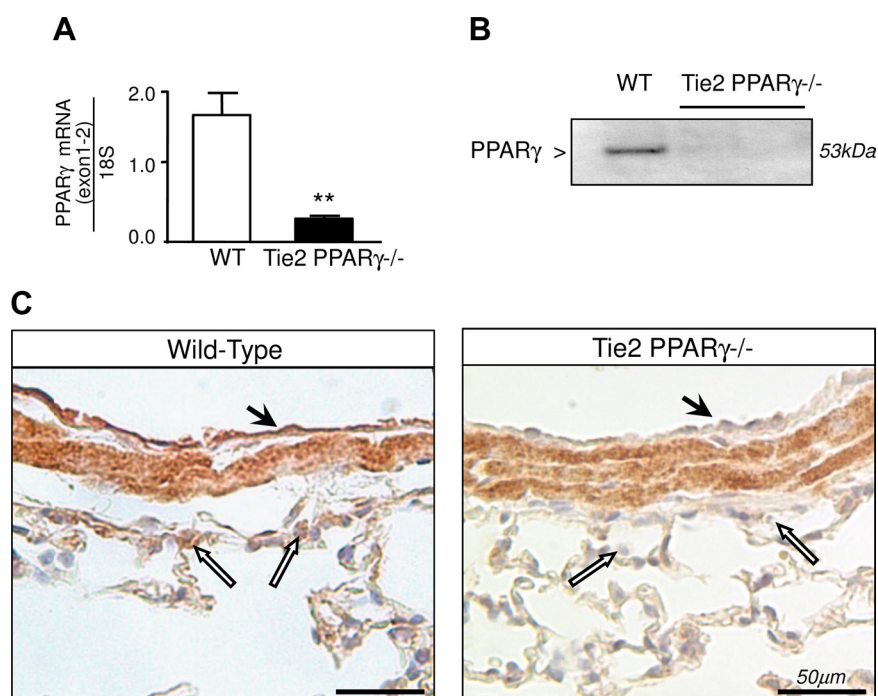


Fig. 1. Peroxisome proliferator-activated receptor (PPAR)- γ mRNA and protein in lungs from Tie2 PPAR γ ^{-/-} and wild-type (WT) littermate mice. *A*: quantitative RT-PCR of PPAR γ (exon 1–2) mRNA normalized to 18S assessed in pulmonary endothelial cells (PECs) isolated from Tie2 PPAR γ ^{-/-} and WT mice (*n* = 3). *B*: representative Western immunoblot of PPAR γ protein in PECs isolated from Tie2 PPAR γ ^{-/-} and WT mice (*n* = 3). *C*: representative photomicrographs showing immunoreactivity of PPAR γ in the ECs (black arrows) and in smooth muscle cells (SMCs) of a large pulmonary artery (PA) as well as in cells occupying the position of alveolar macrophages (white arrows) in a WT mouse (left); immunoperoxidase staining is absent in ECs and alveolar macrophages in a similar section from a Tie2 PPAR γ ^{-/-} mouse (right). Scale bar = 50 μ m.

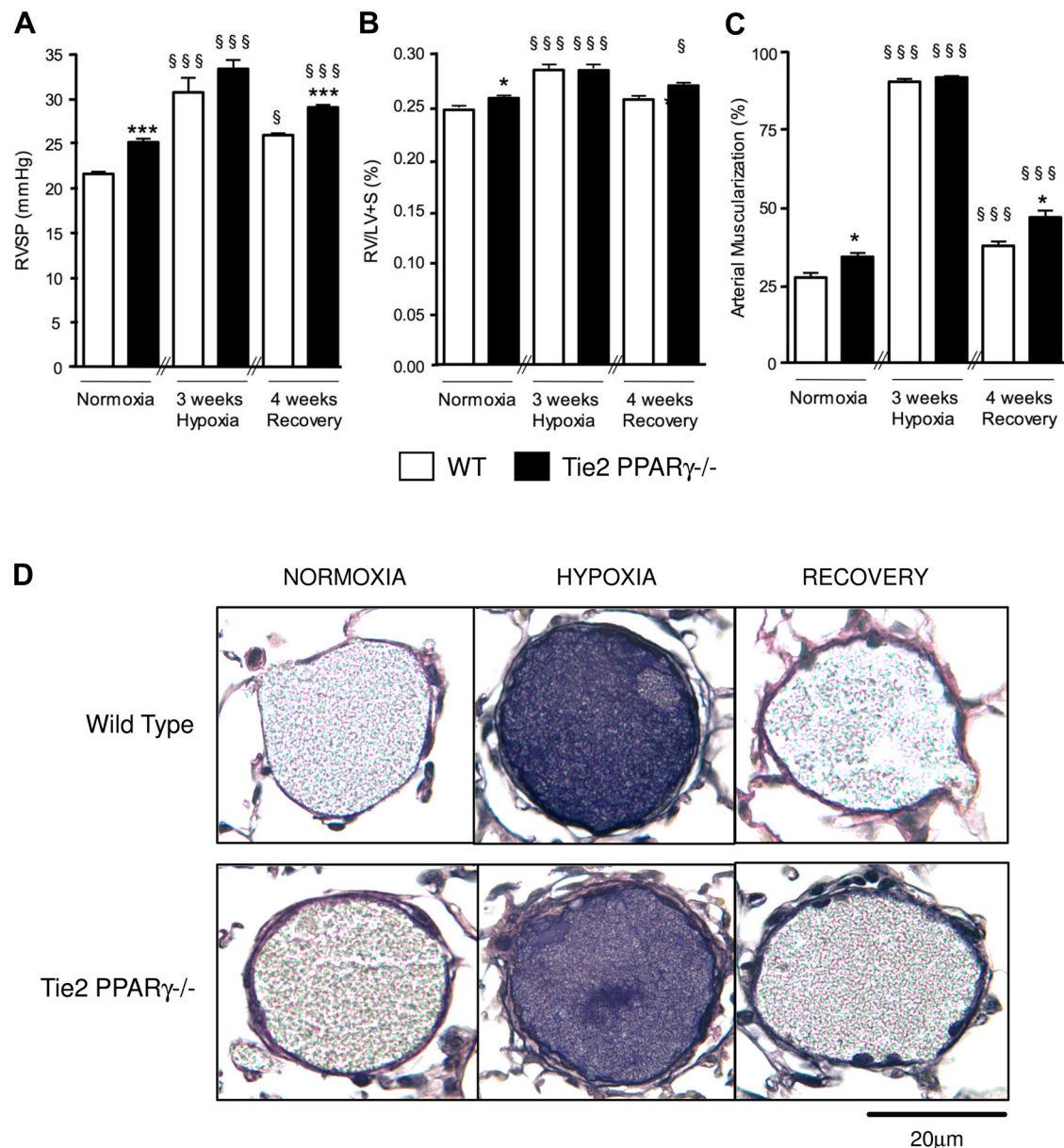


Fig. 2. Right ventricular systolic pressure (RVSP), RV hypertrophy (RVH) [right ventricle/left ventricle plus septum (RV/LV+S)], and percentage of muscularized distal arteries in Tie2 PPAR γ ^{-/-} and WT littermates in normoxia, following chronic hypoxia, and after 4 wk recovery in normoxia. RVSP (A), Fulton index: RV/LV+S (B), and percentage of muscularized alveolar duct and wall arteries (C). D: representative Movat pentachrome stained sections of alveolar duct PAs: muscularized PAs have a double elastic lamina seen in WT only in hypoxia and in Tie2 PPAR γ ^{-/-} under all 3 conditions. Bars are means \pm SE ($n = 10$). * $P < 0.05$, and *** $P < 0.001$, Tie2 PPAR γ ^{-/-} vs. WT; § $P < 0.05$, §§§ $P < 0.001$, hypoxia or recovery vs. normoxia. Scale bar = 20 μ m.

(1% O₂). Similarly Yun et al. (45) reported in 3T3-L1 preadipocytes that hypoxia inhibits the induction of PPAR γ 2 mRNA by Northern blot (45). Therefore, to investigate whether the similar degree of PAH observed between both genotypes following chronic hypoxia could be explained by reduced endothelial PPAR γ expression in WT mice, we performed additional experiments. First, we used Western immunoblots to assess the PPAR γ protein levels in lung homogenates from normoxia and chronic hypoxia exposed WT mice but found no significant differences ($n = 3$ in each group; $P = \text{NS}$; see Supplemental Fig. S1). Then, we assessed the effect of hypoxia (1% O₂ for 24 h) vs. normoxia on the PPAR γ protein level in murine PECs isolated from WT mice. Consistent with our

in vivo results, we found no difference in the PPAR γ protein level in treated or untreated cultured PECs ($n = 3$ in each group; $P = \text{NS}$; see Supplemental Fig. S2).

Tie2 PPAR γ ^{-/-} Mice Have Increased Expression and Activation of PDGF-R β

Exaggerated PDGF-R β -mediated signaling appears to be a key factor in the PASM cell proliferation associated with PAH, including that observed in the SM22 PPAR γ ^{-/-} mice (10, 30, 35). We therefore investigated whether the increased muscularity developing in the Tie2 PPAR γ ^{-/-} mice was the result of increased PDGF signaling by measuring lung proteins levels of

Table 1. Echocardiographic measurements and ratio of number of arteries/100 alveoli in Tie2 PPAR γ ^{-/-} and WT mice

	Normoxia		Chronic Hypoxia		Recovery	
	WT	Tie2 PPAR γ ^{-/-}	WT	Tie2 PPAR γ ^{-/-}	WT	Tie2 PPAR γ ^{-/-}
Heart rate, beats/min	518±56	545±76	517±36	548±24	483±31	464±13
Diastolic BP, mmHg	89.5±6.0	82.2±8.4	79.2±7.4	85.1±7.2	81.3±8.0	85.8±7.8
Mean BP, mmHg	101.8±3.9	96.1±6.8	94.0±0.2	96.4±5.4	90.1±9.4	93.6±7.2
Systolic BP, mmHg	123.2±4.7	117.8±7.4	110.2±8.2	116.2±7.5	108.5±9.9	111.6±9.1
LV fractional shortening	40.93±1.07	42.16±3.60	42.68±5.12	43.09±4.54	41.63±3.07	40.21±3.28
Cardiac output, ml/min	27.13±1.16	27.46±1.45	25.40±2.34	25.34±2.56	27.48±1.70	26.56±2.22
No. arteries per 100 alveoli	1.87±0.25	2.15±0.17	3.27±0.34	3.13±0.31	2.50±0.26	2.76±0.38
n	8	7	7	8	7	9

Data are means \pm SE. WT, wild type; PPAR γ , peroxisome proliferator-activated receptor- γ ; BP, blood pressure; LV, left ventricular.

PDGF-B and the PDGF-R β in the Tie2 PPAR γ ^{-/-} and WT mice. We found that while the level of PDGF-B was similar in both genotypes, the expression of the receptor PDGF-R β was increased by approximately twofold in the lungs of the Tie2 PPAR γ ^{-/-} vs. WT mice in room air. In keeping with the hemodynamic results, similar increases in PDGF-R β were seen in both groups after chronic hypoxia and after recovery in room air (Fig. 3, A and B). Consistent with this observation, more intense immunoreactivity was noted for PDGF-R β in the distal pulmonary artery walls from Tie2 PPAR γ ^{-/-} vs. WT mice by immunohistochemistry (Fig. 3C).

Tie2 PPAR γ ^{-/-} Mice Have Increased Expression of PDGF-R β Despite Increased Expression of ApoE

In looking for a mechanism by which disruption of PPAR γ in Tie2-expressing cells could result in the in-

creased PDGF-R β expression in the PSMCs, we measured levels of the PPAR γ target apoE. ApoE is a transcriptional target of PPAR γ (10), and it can inhibit PDGF-R β signaling (2) and PSMC proliferation (10). We first investigated the ability of apoE to regulate PDGF-R β expression in cultured human PSMCs. We found a dose-dependent inverse relationship between apoE and PDGF-R β expression, with 10 μ g/ml of recombinant apoE significantly decreasing PDGF-R β expression by \sim 35% ($P < 0.01$; Fig. 4A). However, when we determined whether the loss of PPAR γ reduced apoE expression in the transgenic mice, we found that the apoE mRNA level was similar in whole lung homogenates from both genotypes (data not shown) and that apoE protein was increased by approximately twofold in the PECs isolated from the Tie2 PPAR γ ^{-/-} vs. WT mice (Fig. 4B).

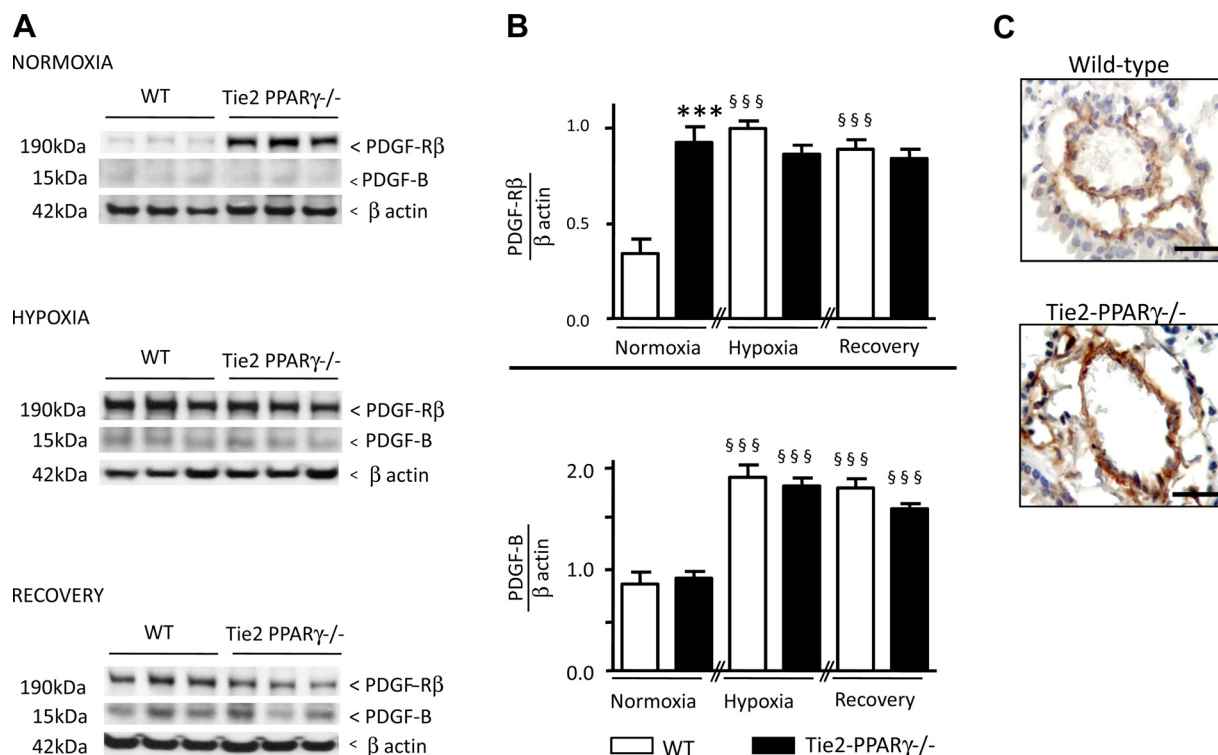


Fig. 3. Platelet-derived growth factor receptor- β (PDGF-R β) and PDGF-B in Tie2 PPAR γ ^{-/-} vs. WT lungs in normoxia, following hypoxia, and after recovery in normoxia. A: representative Western immunoblots of PDGF-R β , PDGF-B, and β -actin loading control in lung homogenates from 3 representative mouse lungs. B: quantification of PDGF-R β , β -actin, and PDGF-B-to- β -actin ratios. C: representative photomicrographs of mouse lung sections from Tie2 PPAR γ ^{-/-} and WT mice in normoxia after immunoperoxidase staining for PDGF-R β . Bars are means \pm SE ($n = 5$). *** $P < 0.001$, Tie2 PPAR γ ^{-/-} vs. WT; §§ $P < 0.001$, chronic hypoxia or recovery vs. normoxia. Scale bar = 50 μ m.

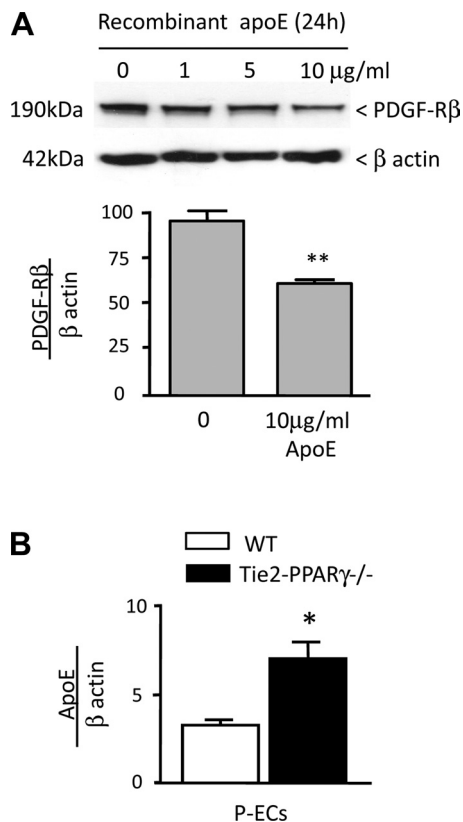


Fig. 4. Effect of recombinant apoE on PDGF-R β in cultured human PASMC and lung apolipoprotein E (apoE) levels in Tie2 PPAR γ ^{-/-} vs. WT mice in normoxia. **A**: representative Western immunoblot showing the PDGF-R β protein:β-actin level in cultured human PASMCs exposed to increasing doses of recombinant apoE for 24 h and quantification of the PDGF-R β -to-β-actin ratio. Bars are means \pm SE ($n = 4-5$). **B**: apoE-to-β-actin ratio in PECs isolated from Tie2 PPAR γ and WT mice. * $P < 0.05$, Tie2 PPAR γ ^{-/-} vs. WT; ** $P < 0.01$, unstimulated vs. apoE-stimulated PASMCs.

Blocking PDGF-R β Signaling Is Sufficient to Prevent the PAH that Develops in the Tie2 PPAR γ ^{-/-} Mice Under Room Air

Although we could not ascribe the increased PDGF-R β expression in the transgenic mice to a reduction in apoE, we next determined whether blocking PDGF signaling would reverse the PAH observed in these animals at baseline. We administered over the course of 2 wk, a daily intraperitoneal injection of imatinib, a competitive inhibitor of PDGF-R β tyrosine kinase activity (35). We demonstrate that treatment with imatinib effectively blocked PDGF-R β signaling in the Tie2 PPAR γ ^{-/-} mice as evidenced by decrease in its phosphorylation (tyrosine 751) and its activity as reflected by phosphorylation of ERK1/2 (Fig. 5, *A* and *B*). Furthermore, this treatment reversed the PAH in the Tie2 PPAR γ ^{-/-} mice, decreasing RVSP, RVH, and muscularization of peripheral arteries to similar levels observed in WT controls (Fig. 5, *A-E*).

DISCUSSION

In our previous studies (10), we showed that PAH develops in mice in which PPAR γ is decreased in SMC, and that PPAR γ acts downstream of BMPR-II signaling. Since PPAR γ is reduced in both the ECs and SMCs of PAH patients (1), we hypothesized that the loss of PPAR γ in ECs might also lead to

PAH. Consistent with the fact that the Tie2 promoter drives expression in both EC and bone marrow-derived hematopoietic cells (17, 40), we found a loss PPAR γ in the ECs of the Tie2 PPAR γ ^{-/-} mice. Although the severity of the PAH under room air conditions was mild, there was associated significant RVH and muscularization of distal arteries. Given that the hemodynamic and structural response to hypoxia was similar in both genotypes, it could be that the mechanism responsible for the baseline PAH observed in the Tie2 PPAR γ ^{-/-} mice in room air may be similar to the one that produces PAH in the WT mice during chronic hypoxia. Indeed, elevated PDGF-R β expression and activation were present in the Tie2 PPAR γ ^{-/-} mice in room air and in both genotypes following chronic hypoxia. Inhibition of this abnormal PDGF-R β activity in the Tie2 PPAR γ ^{-/-} mice in room air with imatinib normalized the hemodynamic and pulmonary vascular remodeling to levels close to those found in WT mice, implicating the increased PDGF-R β activity as one mechanism necessary for the evolution of the PAH in our model. However, the expression of PDGF-R β in the two groups was similar following 4 wk of recovery in room air despite that a persistent increase in PAH severity was observed in the Tie2 PPAR γ ^{-/-} mice upon return to normoxia, suggesting that an additional mechanism is likely responsible for the impaired recovery.

We (10) and others (30, 35) have shown that PDGF-R β -mediated signals drive the PASMC proliferation associated with PAH. PDGF expression increased in lung biopsies obtained from patients with severe PAH (30, 35). In addition, treatment of rats with either monocrotaline- or chronic hypoxia-induced PAH with the PDGF-R β inhibitor imatinib produced a dose-dependent significant improvement of pulmonary hemodynamics and vascular remodeling within 2 wk (35). Given that the PPAR γ expression is intact in the pulmonary vascular SMCs of the Tie2 PPAR γ ^{-/-} mice, the increased PDGF-R β expression and signaling observed in the walls of the distal PAs are likely due to paracrine effects. Endothelial abnormalities and dysfunction in the intercellular communications between ECs and SMCs have been implicated in the pathogenesis of PAH by our group (31) and by others (5, 7, 13, 15, 32). In support of this, a recent study from Hong et al. (13) demonstrated that conditional heterozygous or homozygous BMPR-II deletion in PEC predisposes mice toward the development of PAH and induces a higher proliferation index of both PECs and pulmonary SMCs. As PPAR γ acts downstream of BMPR-II signaling (10), we cannot exclude the possibility that mechanisms causing the spontaneous PAH in our model are similar to those leading to the PAH that develops in mice following ablation of the BMPRII gene in ECs. In addition, similar to BMPR-II, activation of PPAR γ protects the vascular endothelium from inflammation, by decreasing the nitric oxide synthase inhibitor asymmetric dimethylarginine (23, 37, 39), ET-1 (21, 33), and cell surface and secreted molecules related to inflammation such as vascular cell adhesion molecule and fractalkine (25, 36). While inflammatory mediators known to play a role in PAH may be increased and could be an additional mechanism contributing to the pulmonary vascular changes observed, no significant changes in plasma ET-1 levels and nitrate/nitrite productions were seen in the lungs from the Tie2 PPAR γ mice compared with WT mice. Using a similar Tie2-mediated PPAR γ knockout model, Kanda et al. (16) demonstrated that these transgenic mice vs. controls had impaired

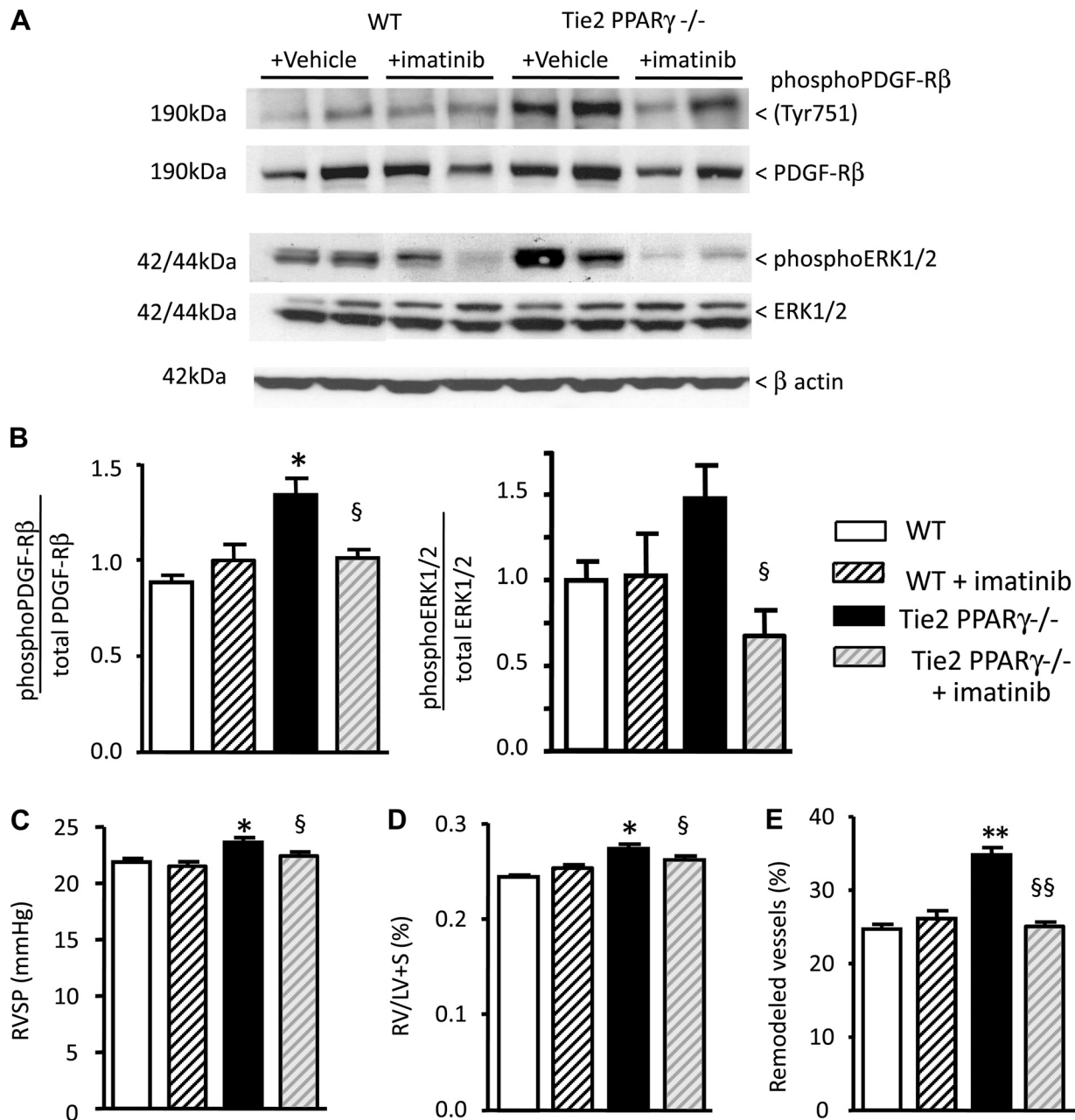


Fig. 5. Lung phosphoPDGF-R β , PDGF-R β , phosphoERK1/2, and ERK1/2 and RVSP, RVH, and muscularized arteries in Tie2 PPAR γ ^{-/-} vs. WT mice following imatinib (50 mg \cdot kg⁻¹ \cdot day⁻¹), or vehicle (isotonic saline) for 2 wk. **A**: Representative Western immunoblots of lung phosphoPDGF-R β , PDGF-R β , phosphoERK1/2, ERK1/2, and β -actin. **B**: quantification of the phosphoPDGF-R β -to-PDGF-R β ratio and phosphoERK1/2-to-ERK1/2 ratio. Bars are means \pm SE ($n = 5$). RVSP (**C**), Fulton index: RV/LV+S (**D**), and percentage of muscularized peripheral arteries (**E**). Bars are means \pm SE ($n = 10$). * $P < 0.05$ Tie2 PPAR γ vs. WT mice; § $P < 0.05$, §§ $P < 0.01$, treated vs. untreated Tie2 PPAR γ ^{-/-} mice.

arterial relaxation only after feeding with a high-fat diet. In contrast, Kleinhenz et al. (18) demonstrated impaired endothelium-dependent vasodilatation in aortic rings following feeding with standard chow diets and found that intact aortic ring segments from Tie2 PPAR γ ^{-/-} mice released less nitric oxide than WT mice. These studies indicate that different vascular beds may have different sensitivities to the loss of EC PPAR γ . While reduced PPAR γ has been demonstrated in human PAECs after 72 h of hypoxia (28), we could not document a similar decrease after 24 h and our cells did not tolerate longer exposures.

In view of our previous report (10) that the spontaneous PAH developing in the SM22 PPAR γ ^{-/-} mice was related to reduced levels of a target of PPAR γ , apoE, we measured apoE levels in the Tie2 PPAR γ ^{-/-} mice. ApoE is a molecule that inhibits PDGF-R β function by binding to low-density receptor-like protein-1 and by activation of the PDGF-R β (2, 14, 26, 47). We demonstrated that the incubation of primary human PASMCs with recombinant apoE resulted in a dose-dependent inverse relationship between apoE and PDGF-R β protein expression. However, we found that the apoE levels were elevated rather than decreased in two different Tie2-expressing

cells in the Tie2 PPAR γ ^{-/-} mice, PECs, and alveolar macrophages (data not shown). Although the precise mechanisms causing the increased expression and activation of PDGF-R β in the Tie2 PPAR γ ^{-/-} mice in room air are not clear, these data suggest that heightened apoE expression, by preventing a further increase in PDGF-R β , might represent a potent protective mechanism against the development of more severe PAH in these mice and might explain the similar severity of PAH observed in chronic hypoxia in the Tie2 PPAR γ ^{-/-} and the WT mice. In our previous studies (10) in which PPAR γ is decreased in SMCs we identified a BMP-mediated increase in apoE that was PPAR γ independent, so it is possible that this pathway compensates for the loss of PPAR γ -mediated apoE.

In summary, although the precise pathophysiological mechanisms explaining the increased expression and activation of PDGF-R β in the Tie2 PPAR γ ^{-/-} mice are not clear, our data demonstrate that loss of endothelial PPAR γ results in PA muscularization and development of PAH. This model of disease supports the hypothesis that endothelial dysfunction plays a central role in the pathogenesis of the structural alterations of the pulmonary vasculature accompanying PAH.

ACKNOWLEDGMENTS

Present address of G. Hansmann: Dept. of Cardiology, Children's Hospital Boston, Harvard Medical School, Boston, MA.

GRANTS

This work was supported by Postdoctoral Fellowships from the Délégation à la Recherche Clinique de l'AP-HP (to C. Guignabert); the Sigrid Juselius Foundation, Instrumentarium Foundation, the Finnish Foundation for Cardiovascular Research, and the Academy of Finland (to T. Alastalo); the Department of Pediatrics of Mie University Graduate School of Medicine, Japan (to H. Sawada); the American Heart Association/Pulmonary Hypertension Association (to N. El-Bizri and G. Hansmann); and National Heart, Lung, and Blood Institute Grants R01-HL074186 and R01-HL087118 and the Dwight and Vera Dunlevie Endowed Professorship (to M. Rabinovitch).

DISCLOSURES

None of the authors have any disclosures related to conflict of interest.

REFERENCES

- Ameshima S, Golpon H, Cool CD, Chan D, Vandivier RW, Gardai SJ, Wick M, Nemenoff RA, Geraci MW, Voelkel NF. Peroxisome proliferator-activated receptor gamma (PPARgamma) expression is decreased in pulmonary hypertension and affects endothelial cell growth. *Circ Res* 92: 1162–1169, 2003.
- Boucher P, Gotthardt M, Li WP, Anderson RG, Herz J. LRP: role in vascular wall integrity and protection from atherosclerosis. *Science* 300: 329–332, 2003.
- Braissant O, Fougelle F, Scotto C, Dauca M, Wahli W. Differential expression of peroxisome proliferator-activated receptors (PPARs): tissue distribution of PPAR-alpha, -beta, and -gamma in the adult rat. *Endocrinology* 137: 354–366, 1996.
- Bull AW. The role of peroxisome proliferator-activated receptor gamma in colon cancer and inflammatory bowel disease. *Arch Pathol Lab Med* 127: 1121–1123, 2003.
- Dewachter L, Adnot S, Fadel E, Humbert M, Maitre B, Barlier-Mur AM, Simonneau G, Hamon M, Naeije R, Eddahibi S. Angiotensin/Tie2 pathway influences smooth muscle hyperplasia in idiopathic pulmonary hypertension. *Am J Respir Crit Care Med* 174: 1025–1033, 2006.
- Duan SZ, Ivashchenko CY, Usher MG, Mortensen RM. PPAR-gamma in the cardiovascular system. *PPAR Res* 2008: 745804, 2008.
- Eddahibi S, Guignabert C, Barlier-Mur AM, Dewachter L, Fadel E, Darteville P, Humbert M, Simonneau G, Hanoun N, Saurini F, Hamon M, Adnot S. Cross talk between endothelial and smooth muscle cells in pulmonary hypertension: critical role for serotonin-induced smooth muscle hyperplasia. *Circulation* 113: 1857–1864, 2006.
- El-Bizri N, Wang L, Merklinger SL, Guignabert C, Desai T, Urashima T, Sheikh AY, Knutsen RH, Mecham RP, Mishina Y, Rabinovitch M. Smooth muscle protein 22alpha-mediated patchy deletion of Bmpr1a impairs cardiac contractility but protects against pulmonary vascular remodeling. *Circ Res* 102: 380–388, 2008.
- Ghosh SS, Gehr TW, Ghosh S, Fakhry I, Sica DA, Lyall V, Schoolwerth AC. PPARgamma ligand attenuates PDGF-induced mesangial cell proliferation: role of MAP kinase. *Kidney Int* 64: 52–62, 2003.
- Hansmann G, de Jesus Perez VA, Alastalo TP, Alvira CM, Guignabert C, Bekker JM, Schellong S, Urashima T, Wang L, Morrell NW, Rabinovitch M. An antiproliferative BMP-2/PPARgamma/apoE axis in human and murine SMCs and its role in pulmonary hypertension. *J Clin Invest* 118: 1846–1857, 2008.
- Hansmann G, Wagner RA, Schellong S, Perez VA, Urashima T, Wang L, Sheikh AY, Suen RS, Stewart DJ, Rabinovitch M. Pulmonary arterial hypertension is linked to insulin resistance and reversed by peroxisome proliferator-activated receptor-gamma activation. *Circulation* 115: 1275–1284, 2007.
- He W, Barak Y, Hevener A, Olson P, Liao D, Le J, Nelson M, Ong E, Olefsky JM, Evans RM. Adipose-specific peroxisome proliferator-activated receptor gamma knockout causes insulin resistance in fat and liver but not in muscle. *Proc Natl Acad Sci USA* 100: 15712–15717, 2003.
- Hong KH, Lee YJ, Lee E, Park SO, Han C, Beppu H, Li E, Raizada MK, Bloch KD, Oh SP. Genetic ablation of the BMPR2 gene in pulmonary endothelium is sufficient to predispose to pulmonary arterial hypertension. *Circulation* 118: 722–730, 2008.
- Ishigami M, Swertfeger DK, Granholm NA, Hui DY. Apolipoprotein E inhibits platelet-derived growth factor-induced vascular smooth muscle cell migration and proliferation by suppressing signal transduction and preventing cell entry to G1 phase. *J Biol Chem* 273: 20156–20161, 1998.
- Izikki M, Guignabert C, Fadel E, Humbert M, Tu L, Zadigue P, Darteville P, Simonneau G, Adnot S, Maitre B, Raffestin B, Eddahibi S. Endothelial-derived FGF2 contributes to the progression of pulmonary hypertension in humans and rodents. *J Clin Invest* 119: 512–523, 2009.
- Kanda T, Brown JD, Orasanu G, Vogel S, Gonzalez FJ, Sartoretto J, Michel T, Plutzky J. PPARgamma in the endothelium regulates metabolic responses to high-fat diet in mice. *J Clin Invest* 119: 110–124, 2009.
- Kisanuki YY, Hammer RE, Miyazaki J, Williams SC, Richardson JA, Yanagisawa M. Tie2-Cre transgenic mice: a new model for endothelial cell-lineage analysis in vivo. *Dev Biol* 230: 230–242, 2001.
- Kleinhenz JM, Kleinhenz DJ, You S, Ritzenthaler JD, Hansen JM, Archer DR, Sutcliffe RL, Hart CM. Disruption of endothelial peroxisome proliferator-activated receptor gamma (PPARgamma) reduces vascular nitric oxide production. *Am J Physiol Heart Circ Physiol* First published August 7, 2009; 10.1152/ajpheart.00148.2009.
- Lane KB, Machado RD, Pauciulo MW, Thomson JR, Loyd JE III, Nichols WC, Trembath RC. Heterozygous germline mutations in BMPR2, encoding a TGF-beta receptor, cause familial primary pulmonary hypertension. *Nature Genetics* 26: 81–84, 2000.
- Li X, Kimura H, Hirota K, Sugimoto H, Kimura N, Takahashi N, Fujii H, Yoshida H. Hypoxia reduces the expression and anti-inflammatory effects of peroxisome proliferator-activated receptor-gamma in human proximal renal tubular cells. *Nephrol Dial Transplant* 22: 1041–1051, 2007.
- Martin-Nizard F, Furman C, Delerive P, Kandoussi A, Fruchart JC, Staels B, Duriez P. Peroxisome proliferator-activated receptor activators inhibit oxidized low-density lipoprotein-induced endothelin-1 secretion in endothelial cells. *J Cardiovasc Pharmacol* 40: 822–831, 2002.
- Merklinger SL, Wagner RA, Spiekerkoetter E, Hinek A, Knutsen RH, Kabir MG, Desai K, Hacker S, Wang L, Cann GM, Ambartsumian NS, Lukanidin E, Bernstein D, Husain M, Mecham RP, Starcher B, Yanagisawa H, Rabinovitch M. Increased fibulin-5 and elastin in S100A4/Mts1 mice with pulmonary hypertension. *Circ Res* 97: 596–604, 2005.
- Mittermayer F, Schaller G, Pleiner J, Krzyzanowska K, Kapiotis S, Roden M, Wolzt M. Rosiglitazone prevents free fatty acid-induced vascular endothelial dysfunction. *J Clin Endocrinol Metab* 92: 2574–2580, 2007.
- Murdoch C, Tazzyman S, Webster S, Lewis CE. Expression of Tie-2 by human monocytes and their responses to angiotensin-2. *J Immunol* 178: 7405–7411, 2007.
- Napimoga MH, Vieira SM, Dal-Secco D, Freitas A, Souto FO, Mestriner FL, Alves-Filho JC, Grespan R, Kawai T, Ferreira SH, Cunha FQ. Peroxisome proliferator-activated receptor-gamma ligand, 15-deoxy-delta-

- 12,14-prostaglandin J2, reduces neutrophil migration via a nitric oxide pathway. *J Immunol* 180: 609–617, 2008.
26. Newton CS, Loukinova E, Mikhailenko I, Ranganathan S, Gao Y, Haudenschild C, Strickland DK. Platelet-derived growth factor receptor-beta (PDGFR-beta) activation promotes its association with the low density lipoprotein receptor-related protein (LRP). Evidence for co-receptor function. *J Biol Chem* 280: 27872–27878, 2005.
 27. Nicol CJ, Adachi M, Akiyama TE, Gonzalez FJ. PPARgamma in endothelial cells influences high fat diet-induced hypertension. *Am J Hypertens* 18: 549–556, 2005.
 28. Nisbet RE, Bland JM, Kleinhenz DJ, Mitchell PO, Walp ER, Sutliff RL, Hart CM. Rosiglitazone attenuates chronic hypoxia-induced pulmonary hypertension in a mouse model. *Am J Respir Cell Mol Biol* 2009 Jun 11. [Epub ahead of print]
 29. Parameswaran N, Hall CS, Bomberger JM, Sparks HV, Jump DB, Spielman WS. Negative growth effects of ciglitazone on kidney interstitial fibroblasts: role of PPAR-gamma. *Kidney Blood Press Res* 26: 2–9, 2003.
 30. Perros F, Montani D, Dorfmüller P, Durand-Gasselin I, Tcherakian C, Le Pavec J, Mazmanian M, Fadel E, Mussot S, Mercier O, Herve P, Emilie D, Eddahibi S, Simonneau G, Souza R, Humbert M. Platelet-derived growth factor expression and function in idiopathic pulmonary arterial hypertension. *Am J Respir Crit Care Med* 178: 81–88, 2008.
 31. Rabinovitch M, Bothwell T, Hayakawa BN, Williams WG, Trusler GA, Rowe RD, Olley PM, Cutz E. Pulmonary artery endothelial abnormalities in patients with congenital heart defects and pulmonary hypertension. A correlation of light with scanning electron microscopy and transmission electron microscopy. *Lab Invest* 55: 632–653, 1986.
 32. Rudic RD, Shesely EG, Maeda N, Smithies O, Segal SS, Sessa WC. Direct evidence for the importance of endothelium-derived nitric oxide in vascular remodeling. *J Clin Invest* 101: 731–736, 1998.
 33. Sakai S, Miyauchi T, Irukayama-Tomobe Y, Ogata T, Goto K, Yamaguchi I. Peroxisome proliferator-activated receptor-gamma activators inhibit endothelin-1-related cardiac hypertrophy in rats. *Clin Sci (Lond)* 103, Suppl 48: 16S–20S, 2002.
 34. Sarraf P, Mueller E, Smith WM, Wright HM, Kum JB, Aaltonen LA, de la Chapelle A, Spiegelman BM, Eng C. Loss-of-function mutations in PPAR gamma associated with human colon cancer. *Mol Cell* 3: 799–804, 1999.
 35. Schermuly RT, Dony E, Ghofrani HA, Pullamsetti S, Savai R, Roth M, Sydykov A, Lai YJ, Weissmann N, Seeger W, Grimminger F. Reversal of experimental pulmonary hypertension by PDGF inhibition. *J Clin Invest* 115: 2811–2821, 2005.
 36. Schmidt S, Moric E, Schmidt M, Sastre M, Feinstein DL, Heneka MT. Anti-inflammatory and antiproliferative actions of PPAR-gamma agonists on T lymphocytes derived from MS patients. *J Leukoc Biol* 75: 478–485, 2004.
 37. Staniloae C, Mandadi V, Kurian D, Coppola J, Bernaski E, El-Khally Z, Morlote M, Pinassi E, Ambrose J. Pioglitazone improves endothelial function in non-diabetic patients with coronary artery disease. *Cardiology* 108: 164–169, 2007.
 38. Tada Y, Majka S, Carr M, Harral J, Crona D, Kuriyama T, West J. Molecular effects of loss of BMPR2 signaling in smooth muscle in a transgenic mouse model of PAH. *Am J Physiol Lung Cell Mol Physiol* 292: L1556–L1563, 2007.
 39. Wakino S, Hayashi K, Tatamatsu S, Hasegawa K, Takamatsu I, Kanda T, Homma K, Yoshioka K, Sugano N, Saruta T. Pioglitazone lowers systemic asymmetric dimethylarginine by inducing dimethylarginine dimethylaminohydrolase in rats. *Hypertens Res* 28: 255–262, 2005.
 40. Wang L, Fuster M, Sriramara P, Esko JD. Endothelial heparan sulfate deficiency impairs L-selectin- and chemokine-mediated neutrophil trafficking during inflammatory responses. *Nat Immunol* 6: 902–910, 2005.
 41. Willson TM, Brown PJ, Sternbach DD, Henke BR. The PPARs: from orphan receptors to drug discovery. *J Med Chem* 43: 527–550, 2000.
 42. Yang LL, Gros R, Kabir MG, Sadi A, Gotlieb AI, Husain M, Stewart DJ. Conditional cardiac overexpression of endothelin-1 induces inflammation and dilated cardiomyopathy in mice. *Circulation* 109: 255–261, 2004.
 43. Yang Q, Li Y. Roles of PPARs on regulating myocardial energy and lipid homeostasis. *J Mol Med* 85: 697–706, 2007.
 44. Yui Y, Hattori R, Kosuga K, Eizawa H, Hiki K, Ohkawa S, Ohnishi K, Terao S, Kawai C. Calmodulin-independent nitric oxide synthase from rat polymorphonuclear neutrophils. *J Biol Chem* 266: 3369–3371, 1991.
 45. Yun Z, Maecker HL, Johnson RS, Giaccia AJ. Inhibition of PPAR gamma 2 gene expression by the HIF-1-regulated gene DEC1/Stra13: a mechanism for regulation of adipogenesis by hypoxia. *Dev Cell* 2: 331–341, 2002.
 46. Zaidi SH, You XM, Ciura S, Husain M, Rabinovitch M. Overexpression of the serine elastase inhibitor elafin protects transgenic mice from hypoxic pulmonary hypertension. *Circulation* 105: 516–521, 2002.
 47. Zeleny M, Swertfeger DK, Weisgraber KH, Hui DY. Distinct apolipoprotein E isoform preference for inhibition of smooth muscle cell migration and proliferation. *Biochemistry* 41: 11820–11823, 2002.

ONLINE DATA SUPPLEMENT

Expanded Materials and Methods:

Experimental Design

We generated mice deficient in PPAR γ in endothelial cells (Tie2 PPAR γ $-/-$), utilizing the Cre-loxP system as previously described (7, 9, 10). Mice expressing Cre recombinase under the control of the Tie2 promoter (5) were bred with mice containing critical exons of PPAR γ flanked by LoxP sites (4) obtained from Jackson Laboratories (Bar Harbor, ME). The offspring genotypes were determined by PCR as previously described (4, 5) and we confirmed that the mice are viable and fertile, and have a normal life span and growth rate. All animal care and procedures were in accordance with the Animal Care Committee at Stanford University following the guidelines of the American Physiological Society.

Tie2 PPAR γ $-/-$ and littermate WT mice were used (n=10/group of each genotype 5 males and 5 females). The mice were studied under room air conditions at 12 weeks of age, or were exposed to hypoxia (10% oxygen) for 3 weeks between 8-11 weeks of age or were exposed to hypoxia and then allowed a period of room air “recovery” for 4 weeks. During the hypoxia exposure oxygen levels were maintained with the ProOx 110 system (BioSpherix), and carbon dioxide levels monitored continuously using the TelAire 7001 monitor (TelAire) as previously described (1).

To assess the impact of heightened PDGF receptor signaling in our mice under room air conditions, we exposed gender matched Tie2-PPAR γ $-/-$ and wild-type littermate mice (5 males and 5 females) to i.p. injections of 50 mg/kg of the tyrosine kinase PDGF- receptor blocker,

Imatinib (LC laboratories, Woburn, MA), diluted in saline, or equal volume of vehicle (isotonic saline) for 2 weeks, based on a previously established protocol (8).

Hemodynamic Measurements and Assessment of Pulmonary Vascular Changes

Right ventricular systolic pressure (RVSP), RV dp/dt and heart rate at were performed in unventilated mice under isoflurane anesthesia (1.5-2.5%, 2L O₂/min.) using a closed chest technique, by introducing a catheter (1.4 F catheter, Millar Instruments Inc, Houston, TX) into the jugular vein and directing it to the right ventricle (13). Systemic blood pressure was determined in conscious animals by a non-invasive computerized tail-cuff method and verified by catheterization of the left carotid artery on mice under isoflurane anaesthesia. Left ventricular (LV) fractional shortening and cardiac output were evaluated by echocardiography using the Acuson Sequoia 256 ultrasound system (Siemens Medical, Mountain View, California) equipped with a high frequency 15-MHz linear transducer (15L8), that offers 0.35-mm lateral resolution and 0.25-mm axial resolution, real-time digital acquisition, storage, and review capabilities (1).

After all the hemodynamic assessments were completed blood was collected by direct cardiac puncture for lipid profile studies described below and the mice were sacrificed by exsanguinations. The heart and lungs were then removed en bloc and right ventricular hypertrophy (RVH) was later evaluated by the Fulton index measurement (right ventricle/left ventricle plus septum RV/LV+S)(6). The pulmonary circulation was flushed with 3mL of buffered saline at 37°C, and then the lungs were either prepared for morphometric analyses (n=5 per group) or the right lung was quickly harvested and immediately snap-frozen in liquid nitrogen and kept at 80°C for western immunoblot analysis and total RNA extraction and the left lung prepared for immunohistochemistry (n=5 per group).

To prepare the lungs for morphometric analyses, the PA was cannulated, and perfused with a warm (60°C) barium-gelatin mixture at 100 cm H₂O pressure, and the lungs were distended by perfusion through the trachea with 10% formalin at a pressure of 20 cm H₂O. Full thickness transverse lung sections were then embedded in paraffin and stained using elastic van Gieson and Movat pentachrome stains. The total number of peripheral arteries was calculated as a ratio of the number of arteries per 100 alveoli in each of 5 to 6 different 20X microscopic fields per section from each lung, and then muscularization was assessed in 15 higher magnification fields/per mouse (X40 magnification) by calculating the proportion of fully and partially muscularized peripheral (alveolar duct and wall) PAs to total peripheral PAs. All morphometric analyses were performed by one blinded observer.

Analysis of Serum Lipids and Lipoprotein Profiles

Heparinized blood samples were collected by right ventricular puncture from transgenic and WT mice at 12 weeks of age. Total cholesterol and triglycerides (Roche Diagnostics), HDL and LDL cholesterol (Wako Diagnostics), were analyzed as well as total protein, glucose, and CO₂ (Stanford Animal Facility Laboratories) to assess any general metabolic effects of PPAR γ deletion in ECs.

Quantitative Real Time-PCR

Total RNA was isolated from frozen lung using Trizol (Invitrogen, Carlsbad, CA), and RNeasy mini kit (Qiagen, Valencia, CA). Total RNA (2 μ g) was reverse-transcribed using Superscript II (Invitrogen, Carlsbad, CA) per manufacturer's instructions. Gene expression levels of PPAR γ (exon1-2) were quantified using pre-verified Assays-on-Demand TaqMan primer/probe sets

(Applied Biosystems, Foster City, CA). The expression level of each gene was normalized to 18S ribosomal RNA using the comparative delta-CT method.

Immunoblotting

Frozen tissue was homogenized, or cells (see below) were lysed in ice-cold RIPA buffer (50mM of Tris-HCl [pH=7.5], 150mM of NaCl, 1% Nonidet P40, 0.5% sodium deoxycholate, and 0.1% sodium dodecyl sulfate) containing a Protease Inhibitor Cocktail (Halt Protease Kit; Thermo Scientific Pierce, Rockford, IL). The protein concentration was determined using protein assay reagent (BioRad, Richmond, CA) following standard protocols and using bovine serum albumin protein standards (Pierce, Rockford, IL). Fifty μ g of protein extracts were resolved on 4-12% NuPage Bis-Tris gels (Invitrogen, Carlsbad, CA), and electrotransferred to PVDF membranes (Hybond-ECL; Amersham Pharmacia Biotech, Buckinghamshire, UK). The PVDF membranes were incubated in blocking buffer (1 \times TBS, 0.1% Tween-20 with 5% [w/v] nonfat dry milk) for 1 hour at room temperature. The membranes were then incubated with primary antibodies for PPAR γ , ApoE (Santa Cruz Biotechnology, Santa Cruz, CA), phosphoERK1/2, total ERK1/2, PDGF B, (Santa Cruz, Santa Cruz, CA), phosphoPDGF-R β (Tyr751) and PDGF-R β (Cell Signaling Technology, Beverly, MA) in primary antibody dilution buffer (1 \times TBS, 0.1% Tween-200 with 1% [w/v] nonfat dry milk) and gently agitated overnight at 4°C. The membranes were then washed with TBS/T and incubated with either sheep anti-mouse (1:1000) or donkey anti-rabbit (1:1000) horseradish peroxidase-conjugated secondary antibodies (Amersham Biosciences, GE Healthcare UK Limited, Bucks, UK) in blocking buffer for 1 hour at room temperature and then washed with TBS/T. Autoradiographs were developed using the enhanced chemiluminescence (ECL) kit (Amersham Biosciences, GE Healthcare UK Limited, Bucks,

UK). Equal loading of protein was confirmed by blotting for β -actin. Relative band strength was determined by densitometry using the public domain NIH Image program (NIH image, ImageJ, <http://rsb.info.nih.gov/ij/>).

Immunohistochemistry

Immunohistochemical staining was performed on lung sections perfused with saline to remove blood and then fixed by perfusion with 10% formalin, and embedded in paraffin. Five μ m sections were placed on Superfrost Plus glass slides and deparaffinized. Antigen retrieval was performed in 10mmol/L of sodium citrate buffer (pH 6.0) heated at 95°C for 20 minutes. The serial sections were pre-treated with 0.1% Triton X-100 [0.1% Triton X-100 in standard sodium (SSC) buffer] for 10 minutes. After blocking endogenous peroxidase activity with a 3% aqueous H₂O₂ solution for 5 minutes, the sections were incubated overnight at 4°C with primary antibodies. The antibodies used and their dilutions were as follows: PPAR γ (1:200) and PDGF-R β (1:500). Labeling was detected with the use of the Vectastain ABC system (Vector Laboratories, Burlingame, CA) following the protocol suggested by the manufacturer, and all sections were counterstained with hematoxylin (Sigma Aldrich, Mountain View, CA).

Nitric Oxide Synthase (NOS) Activity and Endothelin-1 (ET-1) Assays

NOS activity was estimated by the method of Yui et al. (12) in which the stable end-products, nitrate/nitrite (NO_x), were estimated using the Nitric Oxide Synthase Assay Kit (Calbiochem, Catalog# 482702) following the manufacturer's instructions. Plasma endothelin-1 was assessed by enzyme-linked immunosorbent assay (ELISA) as previously described (2, 11).

Cultured Human Pulmonary Artery-Smooth Muscle Cells (PA-SMCs)

The effects of recombinant ApoE protein on PDGF-R β expression were studied in human PA-SMCs obtained from Lonza (Lonza, Walkersville, MD) and cultured according to the manufacturer's recommendation. Growth synchronized cells (following 48h starvation in media supplemented with 0.1% FBS) were exposed to recombinant ApoE (1, 5, and 10 μ g/mL) in serum-free medium for 24 hours before protein extraction, and the expression of PDGF-R β was determined by western immunoblot as previously described (3).

Cultured Murine Pulmonary-Endothelial Cells (P-ECs)

To assess the effect of loss of PPAR γ in the Tie2-expressing cells, the ApoE expression was assessed in cultured P-ECs isolated from the Tie2 PPAR γ and wild-type mice. Murine P-ECs were isolated by digesting whole lung tissue with collagenase IA (0.5mg/ml) for 45 minutes at 37°C. The cell suspension was filtered through 70 μ m filters, and then centrifuged at 250g for 5 minutes. The cell pellet was then washed and resuspended, and EC selectively cultured after incubation with magnetic beads (Dynabeads, Invitrogen, Carlsbad, CA) coated with anti-CD-31 antibody (3). Characterization of the cell culture after isolation was performed by labeling with Dil-conjugated Ac-LDL (Dil-Ac-LDL). Total RNA was extracted from EC from WT and Tie2 PPAR γ ^{-/-} mice with Trizol reagent, cDNA synthesized, and the gene expression of PPAR γ and ApoE determined by quantitative RT-PCR using TaqMan gene expression assays (Applied Biosystems, CA). Total protein was harvested from pooled samples of WT and Tie2 PPAR γ ^{-/-} mice P-EC, and subject to western immunoblot to determine the expression of PPAR γ protein.

Statistical Analysis

The number of animals used in each determination is given in the Figure legends. Values are expressed as mean \pm SEM. In order to determine differences between the Tie2 PPAR γ ^{-/-} and WT mice, unpaired Student t-tests were performed to compare hemodynamics, RVH, vascular changes, protein, and mRNA expressions. Statistical comparisons of the effect of 'Normoxia', 'Chronic Hypoxia', and 'Recovery on hemodynamics', RVH, vascular remodeling, protein, and mRNA expressions in each genotype were performed by One-way ANOVA followed by Bonferroni's post hoc analysis. A *P*-value of 0.05 was considered statistically significant. All statistical analyses were performed with the SPSS 12.0.1 software program (SPSS Inc., Chicago, Illinois, USA).

References:

1. **El-Bizri N, Wang L, Merklinger SL, Guignabert C, Desai T, Urashima T, Sheikh AY, Knutsen RH, Mecham RP, Mishina Y, and Rabinovitch M.** Smooth muscle protein 22alpha-mediated patchy deletion of *Bmpr1a* impairs cardiac contractility but protects against pulmonary vascular remodeling. *Circ Res* 102: 380-388, 2008.
2. **Hansmann G, de Jesus Perez VA, Alastalo TP, Alvira CM, Guignabert C, Bekker JM, Schellong S, Urashima T, Wang L, Morrell NW, and Rabinovitch M.** An antiproliferative BMP-2/PPAR γ /apoE axis in human and murine SMCs and its role in pulmonary hypertension. *J Clin Invest* 118: 1846-1857, 2008.
3. **Hansmann G, Wagner RA, Schellong S, Perez VA, Urashima T, Wang L, Sheikh AY, Suen RS, Stewart DJ, and Rabinovitch M.** Pulmonary arterial hypertension is linked to insulin resistance and reversed by peroxisome proliferator-activated receptor-gamma activation. *Circulation* 115: 1275-1284, 2007.
4. **He W, Barak Y, Hevener A, Olson P, Liao D, Le J, Nelson M, Ong E, Olefsky JM, and Evans RM.** Adipose-specific peroxisome proliferator-activated receptor gamma knockout causes insulin resistance in fat and liver but not in muscle. *Proc Natl Acad Sci U S A* 100: 15712-15717, 2003.
5. **Kisanuki YY, Hammer RE, Miyazaki J, Williams SC, Richardson JA, and Yanagisawa M.** Tie2-Cre transgenic mice: a new model for endothelial cell-lineage analysis in vivo. *Dev Biol* 230: 230-242, 2001.
6. **Merklinger SL, Wagner RA, Spiekerkoetter E, Hinek A, Knutsen RH, Kabir MG, Desai K, Hacker S, Wang L, Cann GM, Ambartsumian NS, Lukanidin E, Bernstein D,**

- Husain M, Mecham RP, Starcher B, Yanagisawa H, and Rabinovitch M.** Increased fibulin-5 and elastin in S100A4/Mts1 mice with pulmonary hypertension. *Circ Res* 97: 596-604, 2005.
7. **Nicol CJ, Adachi M, Akiyama TE, and Gonzalez FJ.** PPAR γ in endothelial cells influences high fat diet-induced hypertension. *Am J Hypertens* 18: 549-556, 2005.
8. **Schermuly RT, Dony E, Ghofrani HA, Pullamsetti S, Savai R, Roth M, Sydykov A, Lai YJ, Weissmann N, Seeger W, and Grimminger F.** Reversal of experimental pulmonary hypertension by PDGF inhibition. *J Clin Invest* 115: 2811-2821, 2005.
9. **Wan Y, Chong LW, and Evans RM.** PPAR- γ regulates osteoclastogenesis in mice. *Nat Med* 13: 1496-1503, 2007.
10. **Wan Y, Saghatelian A, Chong LW, Zhang CL, Cravatt BF, and Evans RM.** Maternal PPAR γ protects nursing neonates by suppressing the production of inflammatory milk. *Genes Dev* 21: 1895-1908, 2007.
11. **Yang LL, Gros R, Kabir MG, Sadi A, Gotlieb AI, Husain M, and Stewart DJ.** Conditional cardiac overexpression of endothelin-1 induces inflammation and dilated cardiomyopathy in mice. *Circulation* 109: 255-261, 2004.
12. **Yui Y, Hattori R, Kosuga K, Eizawa H, Hiki K, Ohkawa S, Ohnishi K, Terao S, and Kawai C.** Calmodulin-independent nitric oxide synthase from rat polymorphonuclear neutrophils. *J Biol Chem* 266: 3369-3371, 1991.
13. **Zaidi SH, You XM, Ciura S, Husain M, and Rabinovitch M.** Overexpression of the serine elastase inhibitor elafin protects transgenic mice from hypoxic pulmonary hypertension. *Circulation* 105: 516-521, 2002.

TABLE S1. Analyses of serum lipids and lipoprotein profiles, and other blood measurements, in Tie2 PPAR γ ^{-/-} mice and WT littermates, in room air (normoxia).

NORMOXIA		
	WT	Tie2 PPAR γ ^{-/-}
Cholesterol (mg/dL)	81.0 \pm 13.5	95.1 \pm 7.7
LDL (mg/dL)	3.0 \pm 1.0	3.3 \pm 0.4
HDL (mg/dL)	55.5 \pm 9.9	65.1 \pm 4.6
Triglycerides (mg/dL)	59.5 \pm 6.0	113.0 \pm 9.1**
Triglycerides/HDL Ratio	1.1 \pm 0.1	1.7 \pm 0.1**
Glucose (mg/dL)*	196.3 \pm 30.1	184.4 \pm 15.1
Total Protein (mg/dL)	3.5 \pm 0.5	4.1 \pm 0.2
CO₂ (mmol/L)	12.2 \pm 1.9	14.6 \pm 0.7
<i>n</i>	4	7

* Glucose measurements were taken under isoflurane, and are therefore high in all groups.

** $P < 0.01$ between the Tie2 PPAR γ ^{-/-} and WT mice

TABLE S2. Analyses of plasma endothelin-1 (ET-1) levels and nitrate/nitrite (NOx) productions in lung homogenates from Tie2 PPAR γ ^{-/-} mice and WT littermates, in room air (normoxia).

NORMOXIA		
	WT	Tie2 PPARγ^{-/-}
ET-1 (fmol/mL)	16,2 ± 2,5	22,3 ± 4,7
NOx (μM/mg of lung tissue)	14.1 ± 1.0	13.3 ± 0.7
<i>n</i>	5	5

FIGURE S1.

Lung PPAR γ levels in WT mice following 3 weeks of chronic hypoxia (HYPOXIA) vs. room air (NORMOXIA). (A) Representative western immunoblots of PPAR γ , and α -Tubulin loading control in lung homogenates from 3 representative mouse lungs. **(B)** Quantification of the PPAR γ : α -Tubulin ratios. Bars represent mean \pm SEM (n=3).

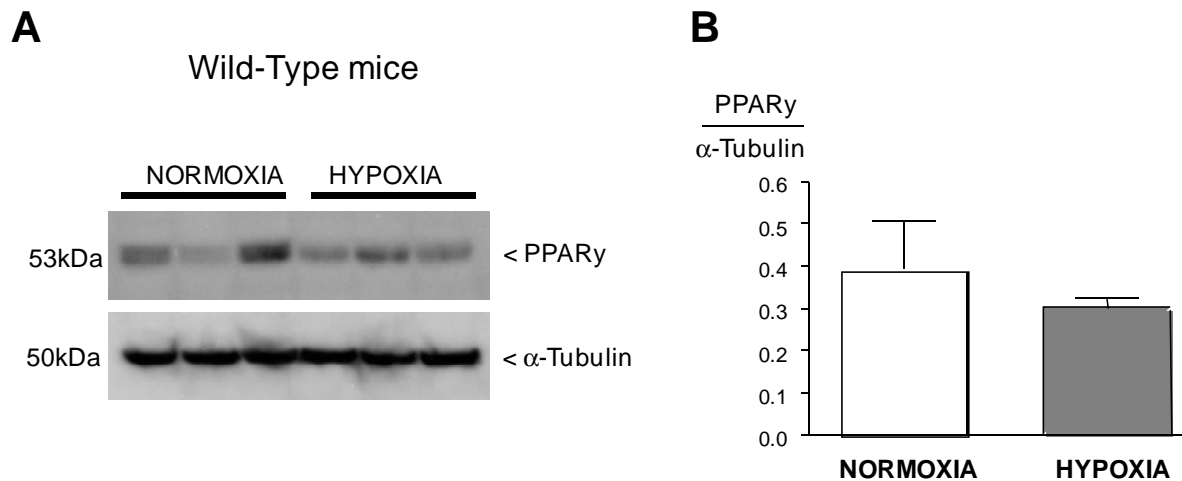


FIGURE S2.

Impact of hypoxia (1% O₂ for 24h) vs. normoxia on PPAR γ levels in murine pulmonary-endothelial cells (P-ECs) isolated from wild-type mice. (A) Representative western immunoblots of PPAR γ , and α -Tubulin loading control level in cultured murine P-ECs exposed to 1% O₂ for 24h. **(B)** Quantification of the PPAR γ : α -Tubulin ratios. Bars represent mean \pm SEM (n=3).

